INSTITUT FÜR PLASMAPHYSIK

GARCHING BEI MÜNCHEN

Ferrite Decoupled Crowbar Sparkgap

R.-C. Kunze, E. v. Mark,
H. Wedler, G. Klement

IPP 4/32 April, 1966

The contents of this report will be presented at the 4th symposium on Engineering Problems in Thermonuclear Research, Frascati-Rome 23 - 27 May, 1966

Die nachstehende Arbeit wurde im Rahmen des Vertrages zwischen dem Institut für Plasmaphysik GmbH und der Europäischen Atomgemeinschaft über die Zusammenarbeit auf dem Gebiete der Plasmaphysik durchgeführt.

IPP 4/32

Ferrite Decoupled Crowbar Sparkgap

G. Klement, R.C. Kunze,
E. v. Mark, H. Wedler

Abstract

The principle of decoupling a crowbar gap using saturable ferrite has been further improved and the trigger mechanism for three switches explained. The design of the first sparkgap is very simple, using a pulse pre-magnetisation, an increase in the available decoupled voltage is achieved. This sparkgap was tested for more than 8000 discharges in a circuit using two units of the 2.6 MJ bank.

The second crowbar switch which also works by the principle of ferrite decoupling, was developed for a 150 kJ bank. Using a third electrode, 2/3 of the ferrite cores can be saved. This electrode is a metal point which for static and dynamic conditions lies at the half potential. The crowbar trigger pulse applied to the point increases the electric field which results in a very early and jitter-free ignition to the main electrode.

The third switch works without ferrite decoupling. The middle electrode, which is a cone shaped electrode as in switch II, breaks down same time to both main electrodes. This is possible, because the trigger pulse on the middle electrode is sharpened through a pulse sharpening gap.

Contents

This report appears in brief, discussion and interpretation of every series of measurements and all tests cannot be made in this conference. A complete report of work on ferrite decoupled and field distortion sparkgaps will appear later.

1.1 Introduction

In plasma physics research, strong magnetic fields are produced by using the pulse-current from a low inductance capacitor bank switched into the inductive load by fast-operating switches (start switches) (fig. H 021a). The plasma lasts for a half-period of the oscillation when it is destroyed by the reversal of the discharge. Without sacrificing the fast rise-time of the field (high frequency), which is very effective in heating the plasma, it is desired to increase the duration-time of the plasma. This is attainable by using a switch which short-circuits the capacitor bank at the first current maximum so that the energy in the load coil is prevented from returning to the bank. Until current maximum the current in the coil is identical with that of the oscillating discharge. From this point in time onwards, the stored magnetic energy in the load coil and therefore the current is exponential with the time constant L/R (fig. H 026, H 033).

A sparkgap which is operated in this way is defined as a "crowbar switch". In crowbar switching one describes the start circuit (capacitor bank - start switches - cables - collector - load coil) and the crowbar circuit (load coil - cables - collector - crowbar switch - and maybe the start switch also) (diagram H 021a).

1.2 Statement of the problem

The following demands are made of the crowbar switch -

1) The ohmic resistance of the switch should not substantially increase the L/R time constant of the crowbarred discharge. The crowbar resistance should not be greater than the resistance of the bank.

2) The ripple of the crowbarred current

from fig. H 033a $R = \frac{I_1 - I_2}{I_1 + I_2} \cdot 100\% \approx \frac{L_{cr}}{L_{load}} \cdot 100\%$

is approximated from the ratio of crowbar switch inductance to load inductance. In order not to exceed a given ripple, the value of the crowbar switch inductance must be achieved which satisfies this ratio. In general the lowest possible ripple is desired.

3) The voltage hold-off of the switch must be greater than the charging voltage of the capacitor bank.

4) At the moment of switching (current maximum), the voltage across the switch is almost zero. Under these conditions the switch must operate with low jitter and take over the current.

5) The switch life should be at least as long as the other components of the bank.

6) Further points to examine are high reliability and simple construction.

From these points crowbar switches for two capacitor banks were developed and examined. Since the working voltage of the banks is 40 kV, it was necessary to use spark-gaps for the switches.

The crowbar sparkgap I, to be described later, is for the 2.6 MJ bank. This bank is divided into 258 single circuits, each being equipt with a start and crowbar sparkgap. A circuit switches 10 kJ and delivers a peak current of 80 kA with a discharge frequency of 25 kc/s. Further data of the circuits are given in the diagram H 023.

The crowbar sparkgap II will be used in a 150 kJ bank which is divided into 28 circuits. In each circuit of the bank a crowbar gap and start gap is used, the crowbar gap being connected before the start gap and direct on the capacitor. A circuit delivers a peak current of 160 kA with a frequency of 93 kc/s. The design of the sparkgap is shown in diagram H 030 which also gives further data.

1.3 Principle of operation

The requirement for the sparkgap to switch at voltage zero is only fulfilled if one electrode is driven to a high voltage by an applied pulse, so that a breakdown is produced between the main electrodes. A reliable ignition will be obtained if the pulse voltage applied to an electrode is 1.5 to 2 times the static breakdown voltage. Such a high voltage is only achieved when the electrodes are sufficiently decoupled.

In most banks the impedance parallel to the crowbar switch is very small, and the decoupling of the electrodes is only attained by using an additional expedient. It would not be possible to drive the electrode E (diagram H 023), using a trigger pulse of usual rise-time and peak voltage, to a voltage high enough to cause breakdown between E and D. A decoupling of both electrodes, by increasing the inductance in the crowbar branch, is to be avoided, which was mentioned at the beginning of the report.

The crowbar inductance should be -

$$L_{cr} \ll L_{sw} + L_{cable} + L_{load}$$

For the crowbar gap I the principle of Kaufmann and Wilhelm (L 1) was used and improved, in which the electrodes were decoupled using saturable ferrite. Using this switch principle the inductance of the crowbar branch will be increased by three orders of magnitude, by insertion of a non-linear, current dependent element. For this crowbar gap, this was achieved using a cylindrical conductor filled with ring-shaped ferrite cores (diagram H 023, H 021a, H 022).

Now it is possible to drive the decoupled crowbar electrode to any high voltage using a trigger pulse, so long as the following conditions are satisfied -

$$H_c \leqq H_{saturation} \qquad (I)$$

$H_{saturation}$ has a characteristic value for each type of ferrite

H_c is the magnetic field strength at the mean radius of the cores.

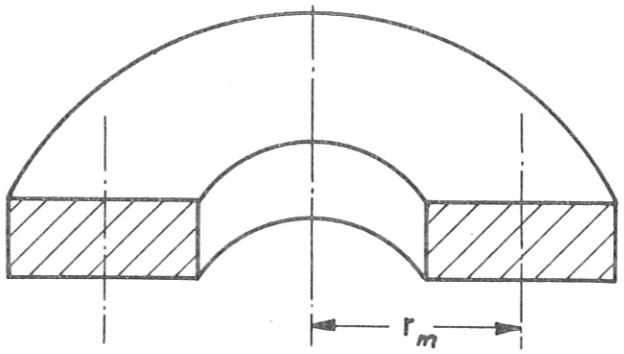

cross section of a ferrite core

The ferrite arrangement is so dimensioned that at the breakdown of point D to E, the ferrite cores are near to saturation, so that during the main breakdown the voltage on the electrode E (the decoupled electrode) will drive them completely into saturation and thereby put a low inductance connection across the capacitor terminals. In the choice of trigger pulse polarity it should be considered that the trigger current and main current flow in the same sense.

1.4 Influence of different sizes of core on the maximum attainable voltage of the decoupled electrode

The relation (I) can be developed further in the following way by considering the condition of the decoupled electrode in the equivalent circuit.

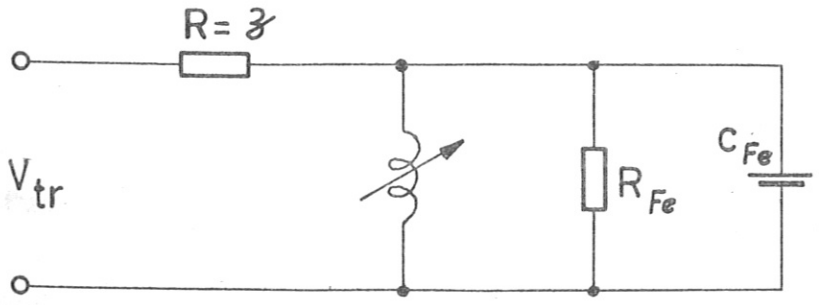

Equivalent circuit of the ferrite arrangement

The impedance of the trigger cable will be represented in the equivalent circuit by an ohmic resistance R. This resistance is so small compared to the ωL of the unsaturated ferrite, that it can be neglected; also the losses in the ferrite cores and stray capacitance, which are represented by a parallel resistance can also be neglected, as shown by analogue measurements.

In this report v_{tr} is given by -

$$v_{tr} = S \cdot t \qquad \text{(II)}$$

where $0 \leq v_{tr} \leq \hat{V}$

S = steepness of the trigger pulse in kV/nsec
t = time in nsec
v_{tr} = voltage on the electrode E (trigger)

$$v_{tr} = L \cdot \frac{di}{dt} \text{ or integrated } \int v_{tr} \cdot dt = Li \qquad \text{(III)}$$

for an approximate solution, L can be considered as a constant.

Neglecting the stray inductance, the inductance of the coaxial ferrite cylinder is given by -

$$L = \mu' \mu_o \cdot 2 \cdot h \cdot n \cdot \log_e \left(\frac{d_a}{d_i}\right) \qquad \text{(IV)}$$

where
h = height of each ferrite core
n = number of ferrite cores
d_a = external diameter of the core
d_i = internal diameter of the core

further
$$H_c = \frac{i}{2 r_m \cdot \pi} \qquad \text{(V)}$$

where r_m = mean radius of core

The maximum attainable voltage on E is given by the condition:

$$H_c = H_{sat} \qquad \text{(1st approximation)}$$

Developing this dependence further and substituting gives -

$$\int v_{tr}.dt = \frac{1}{2}.S.t^2 = L.i = L.H_c.2.r_m.\pi$$

$$\frac{1}{2}.S.t^2 = \mu/\mu_o.4.h.n.\ \log_e(\frac{d_a}{d_i}) \ .\ r_m.\pi\ .H_c$$

$$S.t^2 = 8.h.n.\ \log_e(\frac{d_a}{d_i})\ .\pi\ .\ r_m.\ B_c$$

The time t^x at which the voltage at E breaks down is given by -

$$t^x = \sqrt{\frac{8.h.n.\pi\ .r_m.B_{sat}.\log_e(\frac{d_a}{d_i})}{S}} \qquad \text{(VI)}$$

The maximum attainable voltage on E is -

$$\hat{V}_{tr} = S.t^x = \sqrt{8.S.h.n.\pi\ .r_m.B_{sat}.\log_e(\frac{d_a}{d_i})} \qquad \text{(VII)}$$

Therefore the condition for triggering is given by -

$$\hat{V}_{tr} = \sqrt{8.S.h.n.\pi.r_m.B_{sat}.\log_e(\frac{d_a}{d_i})} > V_{(E-D)pulse} \qquad \text{(VIII)}$$

From which is noted that the pulse breakdown voltage between E and D is a function of the steepness of the trigger pulse -

$$V_{(E-D)pulse} = f(S)$$

To achieve the lowest possible switch inductance, the ratio $\frac{\hat{V}_{tr}}{L_{\text{ferrite arrangement in saturation}}}$ must be as large as possible.

$$\frac{\hat{V}_{tr}}{L_{\text{ferrite arrangement in saturation}}} = \frac{\sqrt{\pi.S.h.n.(d_a-d_i).B_{sat}.\log_e(\frac{d_a}{d_i})}}{\mu_o h.n.\log_e.(\frac{d_a}{d_i})}$$

a = thickness of insulation outside of cores
b = $f(\hat{V})$ = thickness of insulation between cores and bolt.

Therefore in each case S and B_{sat} will be chosen as large as possible. In a construction using the external diameter given, there is then an optimum value of the internal diameter and the number of cores. The cores should not be thicker than 10 mm and an insulating disc should be placed between cores to keep the ferrite loss small.

2. Crowbar sparkgap I

2.1 Statement of the principle

The crowbar gap was triggered using a 2 stage Marx generator with a 40 kV charging voltage (fig. H 024) and delivering 140 kV to the 14 parallel trigger cables (Felten and Guilleaume, type 4.9/17.3; Z_o = 54 ohms, 29 m long). By designing a suitable cable termination using polythene, whose manufacture using a sintering technique will be described in another report, the flash-over length for a 150 kV pulse was limited to 180 mm. This cable-end termination is shown in photograph H 027. The rise of the pulse is 0.5 kV/nsec (diagram H 025a). So with an given number of cores and using this rate of rise of pulse, the attainable voltage on the decoupled electrode E is too low to breakdown the gap. Therefore the electrode E is separated from the trigger cable by a pulse-sharpening gap. With an electrode separation from E - F = 40 mm, the pulse-sharpening gap rises to 110 kV (diagram H 025a), this gives a rate of rise of voltage on the electrode E of 1.5 kV/nsec (diagram H 025c).

From diagram H 025b it is seen that the peak voltage on "E" jitters very badly. This jitter is due to the recovery from the initial magnetic condition of the cores before the arrival of the pulse on "E". The remnance of the ferrite cores is proportional to the extinction current of the last spark and has a different value in each discharge. The peak voltage on "E" is proportional to the working range from the magnetic remnance to saturation.

To sustain a known magnetic condition, the ferrite cores will be premagnetised with the opposite polarity. Hence the trigger pulse

on "F" will be used to feed a premagnetising current via the resistance R_p (diagram H 023, H 024).

The investigation of the most favourable premagnetisation has resulted in a magnetic flux density which is about -80% of that at saturation. Through corresponding choice of the premagnetisation resistor R_p, this premagnetisation can be achieved.

From VIII, the attainable voltage on "E" is proportional to the square root of the rise in flux density (from 0 to B_{sat}). With premagnetisation this is increased by a factor of 1.8 (from -0.8 B_{sat} to B_{sat}). Therefore a theoretical increase in the peak voltage of $\sqrt{1.8} = 1.34$ is achieved.

A comparison of diagrams H 025b and H 025c shows that by using premagnetisation, the jitter of the peak voltage is substantially eliminated. Without premagnetisation the mean value of peak voltage is 61 kV which becomes 80 kV using premagnetisation.

For the main electrodes D and E with diameters of 50 mm and separation of 21 mm, the static breakdown voltage is 62 kV. Applying a pulse factor of 1.33 (without irradiation) gives the requisite voltage on the electrode E of 80 kV. This peak voltage is attained in the described arrangement using 30 ferrite cores from the firm Krupp, type D1S2, with the dimensions 50 mm o.D x 15 mm i.D x 10 mm thick.

The crowbar sparkgap breaks down from E to D at 70 kV so that a safety factor of 10% is given. The lower pulse breakdown voltage is explained by the intense irradiation of the main gap by the discharge at the pulse-sharpening gap. This radiation ensures correct timing and operates only when the crowbar is triggered, so that the voltage hold-off of the crowbar gap is not reduced for the oscillating discharge.

2.2 Mechanical design

The geometrical design of the crowbar gap I was largely dictated by the available room and the arrangement of the start gaps installed in the 2.6 MJ bank. The electrode "D" which is shown in diagram H 021b and H 022 is connected to the load cables by a copper sheet, while the electrode "E" is mounted on the bolt of a coaxial arrangement within which lie the ferrite rings. The bolt of this coaxial system is hollow to allow the premagnetisation. The electrode "E" maintains the trigger pulse over the pulse-sharpening electrode F, which is so arranged that the separation F - D is greater than F - E. The trigger cable and premagnetisation resistor R_p are connected to the electrode "F".

Brass was chosen as the electrode material but the insulation surfaces became heavily contaminated. A test using steel electrodes (Thermax), however, gave unsatisfactory results because points were formed on the electrode surfaces and caused breakdown. Copper was finally chosen as the electrode material and tested for 8000 discharges with a peak current of 80 kA and $\int i\,dt$ of 12 C (diagram H 026a). The erosion of the electrode was evident (diagram H 027a) but after 8000 discharges it did not impair the functioning of the switch.

2.3 Evaluation of the waveforms

From the diagram H o23 of the oscillating discharge the values of resistance and inductance are -

L_{cap}	= 0.022	/uH ;	R_{cap}	= 10	m	(capacitor)
L_{sw}	= 0.20	/uH ;	R_s	= 1.3	m	(start gap)
L_c	= 0.25	/uH ;	R_c	= 11.5	m	(cable)
L_l	= 2.6	/uH ;	R_l	= 1	m	(load)
L_{cr}	= 0.19	/uH ;	R_{cr}	= 9	m	(crowbar)
L_{con}	= 0.14	/uH ;	R_{con}	= 2	m	(connection)

$$f = 25 \text{ kc/s} \qquad \hat{I} = 80 \text{ kA}$$

From diagram H 026a, the crowbar decay time constant is 190 usec. The ripple of the crowbarred current is taken from diagram H 026b -

$$R = \frac{I_1 - I_2}{I_1 + I_2} \times 100\% = 11.9\%$$

The corresponding approximation to the value is -

$$\frac{L_{cr} + L_{con}}{L_1 + L_c} \times 100\% = 11.6\%$$

The diagram H 026b and H 026c each show 20 discharges, before and after a life test. On the upper trace (the load current) demonstrates the operation of the crowbar gap.

When the trigger pulse is applied to the electrode "E" the voltage rises from 0 to 80 kV in 50 nsec (diagram H 025c). The earliest possible breakdown of the gap is when the voltage on "E" has reached the value of the static breakdown voltage E - D = 62 kV. If the voltage on "E" reaches 80 kV, then the ferrites become saturated and the voltage on "E" collapses, hence the gap must breakdown before this time. Therefore the breakdown time must lie within the time in which the voltage on "E" rises from 62 kV to 80 kV. With a pulse rise of 1.5 kV/nsec this is about 12 nsec, giving a jitter t=$\pm$ 6nsec. From the diagrams H 025a, b and c, the jitter of the Marx generator must be subtracted.

It is *not* possible for the trigger pulse to breakdown the gap outside the defined period. An ignition with jitter greater than $\pm$ 6 nsec plus the jitter of breakdown F - E would not result in the reproducable crowbar discharges shown in H 026b and H 026c, which were taken by an automatic camera during the whole of the 8000 shot life test, hence showing that this is not the case. The second trace on diagrams H 026b and c is the crowbar switch current which has the same polarity as the load current (trace 1). In the diagram H 026a the presentation is correct but for the second trace a different amplification was chosen making it only qualitative.

2.4 Switch range

In the section on the principle of the switch it is already stated that the trigger and main current must flow together. This condition gave rise to an enquiry into the switching range. With the capacitor charged to +40 kV (V_c) and using a negative trigger pulse, the crowbar gap can be reliably operated in the range from +40 kV to -4 kV. This corresponds to a switch range of from 0 to ($\frac{T}{4}$ + 600nsec) for a discharge frequency of 25 kc/s.

With a positive trigger pulse, the triggerable voltage range is from +4 kV to $-V_c$ and also from $-V_c$ to +4 kV. This corresponds to a switch range of, from ($\frac{T}{4}$ - 600 nsec) to ($\frac{3}{4}$ T + 600 nsec).

An evaluation of this switch I will be given at the end of the report when the switches I and II will be compared.

3. Crowbar gap II

3.1 Statement of the problem

For the 150 kJ bank described in section 1.1, the user has specified a ripple of less than 20%. If the crowbar gap I were to be used in this bank it would result in a ripple of 50%, from the diagram H030 and the relation

$$R = \frac{L_{cr}}{L_{load}} \times 100\ \%$$

A test of this gap in the circuit confirmed this expectation (diagram H 033a; R = 48%). A reduction of the ripple is possible by using two of the gaps in parallel. It is shown in diagram H 033b that, as expected from the above relation, the ripple is halved (diagram H033b; R = 24%). The 20 discharges on this photograph demonstrate that two or more gaps of this type can be operated in direct parallel connection, without additional time decoupling, taking over the current without mentionable jitter. Using this principle it is possible to build start switches which are not decoupled, but this will not be discussed in this report. For the case in question, the cost of parallel operation of crowbar gaps was too high and a solution will be sought using a ferrite decoupled gap with a centre-electrode.

3.2 Mechanical design (diagram H 028, H 029)

The electrode D is connected to the charging terminal of the capacitor using a parallel plate line. The separation between the electrodes D and E is 21 mm. The electrode E is mounted in the same way as in the crowbar gap I, that is on the bolt of a coaxial arrangement. The cylinder of this arrangement is connected to the capacitor earth terminal by a parallel plate line.

It will be seen from photograph H 029, that the premagnetisation resistance is encapsulated in a side wall, to which the electrode F and the trigger cable are secured. The opposite side wall is for the two other switch resistances and to the top of this side wall the electrodes H and G are connected. The electrode H lies opposite to the electrode F with a separation of 10 mm. The electrode G is the centre electrode between D and E with the separations E - G = 13 mm and D - G = 10 mm.

The inclusion of the switch elements in the side walls has made a compact switch design possible. The polythene insulation plate above the coaxial arrangement will be so formed that the flash-over path between D and E will be 24 mm longer and that a leakage current must flow against the field (diagram H 028).

3.3 Principle of operation

The principle of operation of the crowbar gap is explained in diagram H 030.

The 1.1 µF capacitor in the trigger circuit is charged to +40 kV and discharged into 28 parallel cables each 15 m long, at the desired crowbar time (usually current-maximum). The pulse at the unterminated end of the cable is rectangular, having the following data - peak voltage -75 kV, rise time (10% - 90%) = 300 nsec. With the trigger generator it is possible to supply the 28 crowbar gaps with the requisite pulse, the trigger cable being connected to the electrode F.

As in crowbar gap I, the ferrite cores will also be premagnetised using the trigger pulse. Using the pulse shape described, results in a premagnetisation resistance of 3 kΩ to approximate to -80% of the saturation flux-density. The trigger pulse on F rises to -4o kV in 140 nsec and at this voltage breaks down the gap F - H = 10 mm. This breakdown causes a discontinuity in the voltage waveform on F which can be seen in oscillogram H 031a and also in the drawing of the idealised waveforms (fig. H 032).

The electrode H is connected to the case of the capacitor(middle potential)by the resistors 2 kΩ and 10 kΩ , across which the trigger pulse is developed after the breakdown of F to H.

In 40 nsec the electrode G is driven to -30 kV (fig. H 031b), which corresponds to the resistance division $\frac{10\ k\Omega}{12\ k\Omega}$ The shape of the electrode G is conical and a very high field stress is produced at its point which causes the breakdown of G to D. The potential on G falls to zero, (switching at current maximum ≈ voltage passing through zero) the 2 kΩ resistance prevents the breakdown of H and F. The voltage on F rises further to -51 kV, when a breakdown between F and E results. By decoupling the electrode E using 10 ferrite cores, it is driven to a maximum voltage of -45 kV. Because of the intense irradiation of the gap G - E by the arcs between F - E and G - D, the electrode E breaks down to D at approximately-35 kV (fig. H 031 G). Therefore the connection E - G - D is made and the switch can conduct.

3.4 Special features of the crowbar switch II

The gap D - E is divided into two branches by the centre electrode G. This leads to a reduction of the triggering voltage required. A maximum voltage of 45 kV at the decoupled electrode E is now sufficient to produce the breakdown between E and D. The number of ferrite cores required can be reduced from 30 to 10. The $\int$voltage.time to breakdown in the crowbar switch I is 2100 kV ns, whereas in version II it is only 700 kV ns and this crowbar branch inductance is 65 nH, divided as follows -

Inductance of spark-gap	29 nH
Inductance of the ferrite configuration (cores in saturation)	29 nH
Inductance of the connections	7 nH

Since the electrode G should be prevented at all costs from igniting to E, the separations G - E and G - D are set asymmetrically (G - E = 13 mm; G - D = 10 mm). This setting is possible because the design of the equipment in sandwich conductor technique causes the electrical field to be asymmetric. This asymmetry can be clearly seen in the field pattern (p. 15). In connection with this equipotential field it should be noted that the measurements were not made on a spatial field, but on a plane one. The dielectric constant of polythene, which is different from 1 ($\varepsilon = 2.3$), was also neglected. The electrode G is located at the centre equipotential surface both in static and ringing operation. Thus, the centre electrode cannot cause any distortion of the field without a triggering pulse.

If the triggering pulse appears at the cone-shaped electrode G, extremely high field strengths ($\sim$ 200 kV/cm) occur at the apex of the electrode and immediately in front of it. There is therefore a possibility of electrons issuing from the tip due to field emission. At any rate, a corona appears at the tip prior to the breakdown proper and consequently numerous electrons and ions as well. In addition, very hard UV radiation is emitted, which in turn uniformly preionizes the two sparkgaps (G - D; G - E). For these reasons the gap G - D will ignite with small jitter and at low pulse voltages.

On ignition current of about 20 A flows in the channel D - G. The apex of the cone allows the photons to penetrate the space G - E without hindrance. The effect is particularly intense because this space is irradiated from the axial direction by the discharge G - D. Electrons and ions can also diffuse freely into the space G - E.

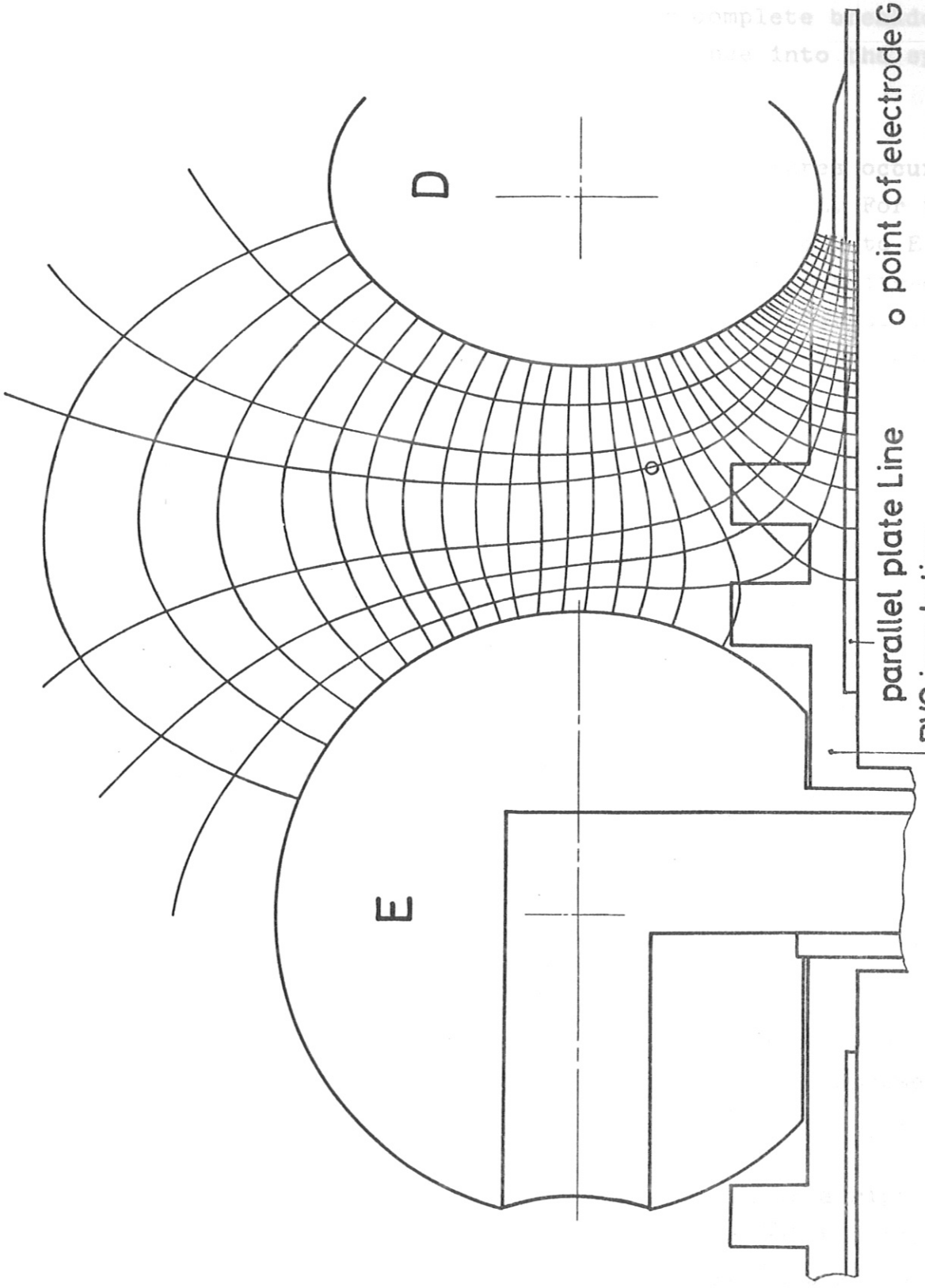

Switch II: Equipotential field measured on a plane model
The dielectric constant of polythene (ε = 2.3) was neglected.

Since the voltage requires about 30 ns for complete breakdown after G - D is ignited, leaders and streamers advance into the space G - E in this time.

When the discharge to D takes place high temperatures occur at the tip which will further assist the breakdown of G - E. For the reasons just mentioned there is a very early breakdown from G to E (35 kV at a separation of 13 mm) when the voltage at the ferrite-decoupled electrode E increases. Even after a number of discharges the peak performance is maintained because the apex of the cone burns down completely uniformly.

Pulse factors (neglecting radiation):

G→D (10 mm) $V_{d\ stat}$ = -20 kV; $V_{tr\ max}$ = -75 kV; α = 3.75;

G→E (13 mm) $V_{d\ stat}$ = +13 kV; $V_{tr\ max}$ = +45 kV; α = 3.45;

F→H (11 mm) $V_{d\ stat}$ = -30 kV; $V_{tr\ max}$ = -75 kV; α = 2.5 ;

F→E (25 mm) $V_{d\ stat}$ = -60 kV; $V_{tr\ max}$ = -75 kV; α = 1.25;

(pulse factors valid for rectangular pulses)

The high pulse factors together with the short rise times cause the sparkgap to work with little jitter. The jitter could be reduced even more if the gap F - E were exposed to more radiation by means of an ignitor.

3.5 Evaluation of the oscillograms

The oscillograms of Fig. H 031a, b, c show the voltage distributions at the electrodes F, E, G. In Fig. H 032 these are represented together in an idealised form.

Evaluation of the oscillogram in Fig. H 033c shows a ripple of the crowbar current of 17.5%. From the relation $R = \frac{L_{cr}}{L}$ the ripple is calculated to be 17.3 %. The oscillogram represents 20 reproducible crowbar discharges.

The jitter can be estimated from the information given in 2.3, according to which a jitter of $\pm$ 9 ns can be expected. The jitter of the pulse sharpening sparkgap F - E is not included in this figure, which thus represents only the time jitter of the breakdown from E to D.

3.6 Switching range

At a discharge frequency of 93 kc/s and a charging voltage of +40 kV the switching range of the crowbar sparkgap II is:

with negative triggering pulse

from V_c = + 40 kV to -3.5 kV, which corresponds to
from t = 0 to ($\frac{T}{4}$ + 150 ns)

with positive triggering pulse

from V_c = + 3.5 kV to -40 kV, which corresponds to
from t = ($\frac{T}{4}$ - 150 ns) to $\frac{T}{2}$

The switching range will exceed $\frac{T}{2}$, but no further extension was determined.

4. Measurements on ferrite cores

In order to keep the inductance of the ferrite configuration at a given $\hat{V}$ as small as possible, 10 different types of ferrite cores were investigated to find the maximum voltage. In this connection the amplitude jitter could largely be avoided by demagnetizing the cores beforehand with a damped ringing discharge. For the same reason no use was made of the pulse sharpening electrode.

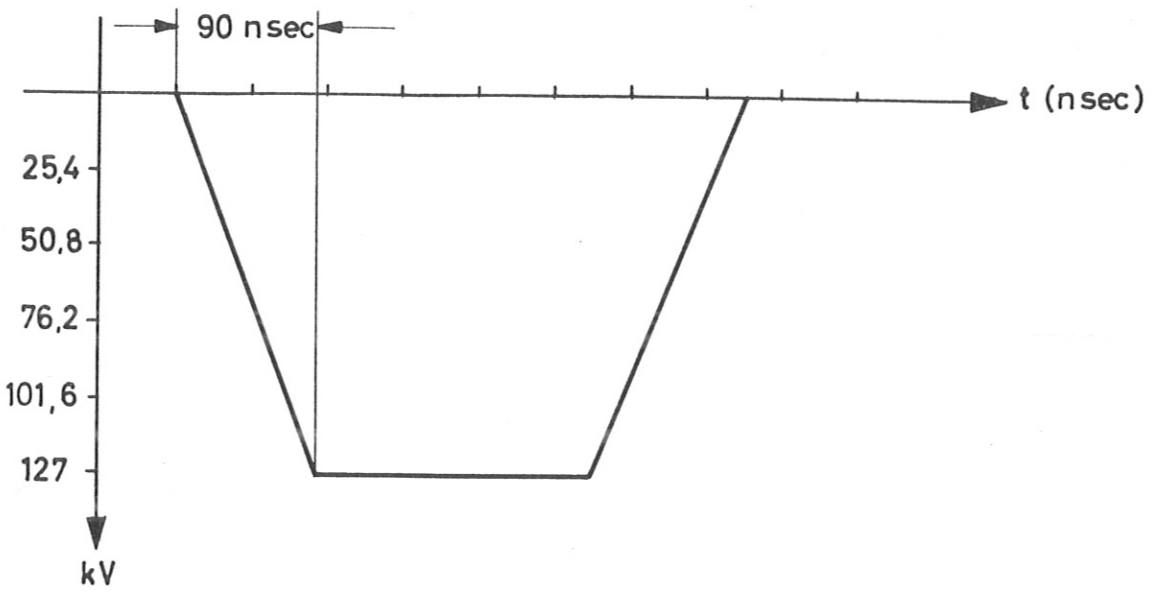

Voltage distribution at the unterminated cable end

The voltage pulse, as represented in idealized form, was applied directly to the ferrite configuration from a 29 m long pulse cable (Z_o = 54 Ω). The maximum voltages reached are plotted in Fig. H 034, where each point plotted is the mean value obtained from 5 measurements. The dimensions and data of the cores are listed in the table on p. 25. The investigations show that the Krupp D1S2 cores used rank with the best.

The approximation $\hat{V}$ = f(n, d_a, d_i, premagnetization) derived on pages 5 to 7 agrees closely with the measured results (an exact evaluation of the measured results is being prepared).

In conclusion, it should be mentioned that the inductance of the ferrite configuration for both switches can be reduced by choosing different core sizes and, possibly, by using more favourable types of core.

For version II a ferrite configuration with the following data was tried out:

Number of cores: 10
Krupp D 1S ; 56 x 32 x 12.5 mm
Maximum voltage attained: $\hat{V}$ = 45 kV

Inductance of the ferrite configuration (in saturated state): 16.5 nH

With these cores it was possible to reduce the saturated ferrite inductance by almost half.

5. Comparison between sparkgaps I and II

Both sparkgaps are suitable for switching high energies (10.6 and 5.3 kJ respectively) and high peak currents (80 and 160 kA respectively). It is worth noting that the charge $\int i dt$ is 12 and 5.5 C respectively. It is therefore obvious that version I, which was used for 8000 discharges, switches more reliably because it works with only 2 main electrodes. Both sparkgaps can be triggered over a wide range with small jitter.

The high voltage pulses (110 kV) at sparkgap I gives rise to quite a number of insulation problems.

In version II it was possible to reduce the inductance of the switch to that of conventional sparkgaps. This was accomplished by using a centre electrode (apex of cone) which also provides for strong field distortion and intense radiation when triggered by a pulse.

A special feature worth mentioning is that both sparkgaps break down at a voltage difference = 0 volt and can therefore work in parallel operation without any transit time decoupling. For this reason the jitter ceases to have the superordinate role that it has in conventional switches.

Data of crowbar sparkgap I and II	I	II
Static breakdown voltage	62 kV	56 kV
Peak current with 40 kV charging voltage	80 kA	160 kA
Energy	1o.6 kJ	5.3 kJ
Charge $\int$idt	12 C	5.5 C
Life test	8000	
Inductance of the sparkgap	70 nH	29 nH
Inductance of the ferrite arrangement	120 nH	29 nH
Inductance of the connections	140 nH	7 nH
Total inductance of the crowbar branch	330 nH	65 nH
Total resistance of the crowbar branch	11 mΩ	5 mΩ
Used on the projected bank		
Ripple	12 %	17.5 %
Rise time of current pulse ($\frac{T}{4}$)	10/us	2.5/us
Decay time constant	190/us	50 /us
Spannungszeitfläche $\int$vdt	2100 kV/nsec	700 kV/nsec
Number of ferrite cores: Krupp D1S2, 50x15x10mm	3o	10
Maximum voltage on the electrode E	80 kV	45 kV
Trigger energy	40 J	10 J
Voltage of the trigger generator	80 kV	40 kV
Withstand voltage of the switch	110 kV	55 kV
Total volume		2200 ccm
Number of main electrodes	2	3
Number of auxiliary electrodes	1	2
Number of auxiliary elements	1	3

With a suitable choice of ferrite cores (dimension, type) combined with a pressure sparkgab it is possible to reduce the inductance even more in both cases and increase the static breakdown voltage.

6. Sparkgap III

6. 1 Basic circuitry

Because of the good experience gained with sparkgap II there was an obvious case for developing a switch capable of switching without ferrite decoupling at low voltages. Unlike version II, in which the gaps D - G and G - E have to be broken down in succession, the intension in the case of type III is to achieve a simultaneous breakdown from the tip G to the two main electrodes D and E.

In principle, it appears possible to effect breakdown to 2 different electrodes. The following conditions have to be observed, however:

1) Sharp triggering pulse (this is achieved with pulse-sharpening gap and matching with a small capacitor, like used by swinging cascade gap),

2) High pulse factor (this is achieved with the sharp triggering pulse, the form of the middle electrode (apex of cone) and no photoemission),

3) Triggering source with small impedance so that the voltage is maintained as long as possible after breakdown. This requirement is met by matching with a 500 pF capacitor (circuit diagram),

4) The pulse breakdown voltages D - G and E - G should be equal if possible. The optimum switching time is then about 0 kV.

Since points 1 and 2 gurantee a high pulse factor it can be assumed that the original avalanche breaks down the gap. If the two decisive avalanches start at different times the second one to start can be assisted so much by using a conical tip (page 14) that it is still able to cover the entire gap. Another point to be noted is that the voltage does not break down until a few nsec after the first avalanche reaches the anode. This means that the avalanche starting later should have plenty of time to develop fully.

Point II should be explained. Usually spark gaps works with very intense irradiation, therefore the gaps break down with low pulse factors and simultaneous ignition is doubtfull. We presume, that a field

emission is more favorable. The electrons are liberated from discrete points and it is probable that the two avalanches develope simultaneously. Further the emission grows explosively.

The high field causes the ionisation coefficient to be increased by ten times. The critical avalanche is developed after 2 mm, therefore built up time is considerably reduced. The high field strength makes the simultaneous development of the two avalanches almost independent of the electrode voltage.

This principle is especially suited for pressurized spark gaps, because field emission is stronger.

The operation of the sparkgap can be understood from the following circuit diagram. The triggering pulse is obtained from the same trigger generator as was used for switch II.

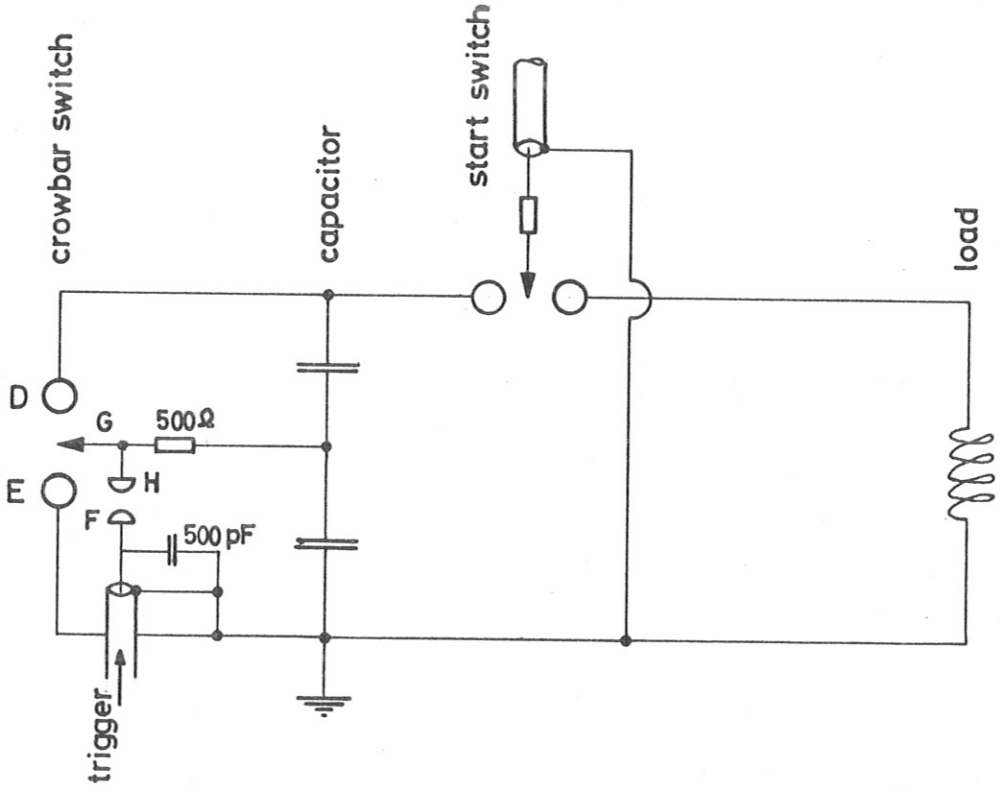

Basic circuit diagram: sparkgap III, used as crowbar switch

Separations set:

Main gap D - E = 20 mm

D - G = E - G = 10 mm

Pulse sharpening gap = F - H = 20 mm

6.2 Use as starting switch

Sparkgap III works at charging voltages down to 100 V. An attempt was made to measure the jitter at such voltages. At a charging voltage of 2 kV the jitter is approximately $\pm$ 30 nsec. This series of

measurements was nevertheless discontinued because the ratio of interference to effective signal was too large. This difficulty could not be eliminated in the time available before the Conference.

6.3 Use as crowbar switch

The picture on sheet H $034/_2$ show crowbar discharges (5 discharges on each). The ignition time is displaced by 100 nsec from one oscillogram to the next.

No jitter can be detected in picture a), ignition time 200 nsec before the current maximum. In the following oscillograms, on the other hand, there is a distinct jitter, which is of the order of about $\pm$ 50 nsec.

It can be assumed that the centre electrode was not set completely symmetrically. The optimum switching time therefore slightly precedes the current maximum. It is supposed that this type of switch near zero kV has a narrow switching range with small jitter. This switching range can, however, be increased by means of suitably sharp triggering pulses and high pulse factors because it is then possible to neglect the voltage at the main electrodes.

A conclusive explanation of this question is expected to emerge in the course of subsequent measurements. In principle, this type of switch can be used as a starting, crowbar or diverting switch.

Literature:

1 R. Wilhelm, H. Zwicker (Zeitschrift für angewandte Physik, 19. Band, 5. Heft, 1965) "Über eine einfache Kurzschluß-Funkenstrecke für Stoßstromanordnungen"

This work was performed under the terms of the agreement on association between the Institut für Plasmaphysik and EURATOM.

Type of core	Symbol	Curve	Firm	Height h mm	Diameters outer mm	Diameters inner mm	μ_A	ϱ Ωcm	B_{1o} gauss	B_{rem} gauss	H_c A/cm	$B_{saturation}$ gauss	$H_{saturation}$ A/cm	f_{max} kc/s
LN	×	I	Mitsubishi	70	24	10	800	500	4000	2000	0.3			500
LN	o	II	Mitsubishi	49.8	19.9	10.3	800	500	4000	2000	0.3			500
LC	•	III	Mitsubishi	49.3	19.6	9.8	200	$5x10^4$	2300	1200	0.8			$2x10^3$
LS	⊡	IV	Mitsubishi	50.5	20.1	10	500	$5x10^5$	2800	1800	o.5			$1.5x10^3$
LM	⊠	V	Mitsubishi	50.7	2o.2	10.1	1000	$1x10^2$	3300	1200	o.2			500
D 1S2	⊕	VI	Krupp	50	15	10	2400 ± 20%	150	4300		0.15	4100	5	300
E 1	⊙	VIII	Krupp	52	15	10	2000	1000	2800..3000		0.25	25oo	5	150
E 2	#	VII	Krupp	50	14.4	10	1000	10000	2600..2800		0.30	3300	5	500
2000 T26	▲	IX	Siemens	72	30.5	5	2200	100			0.2	3700	4	200
3 E 1	⊠	X	Valvo	36.2	23	15	2700		3600			3500	4.5	3 mc/s

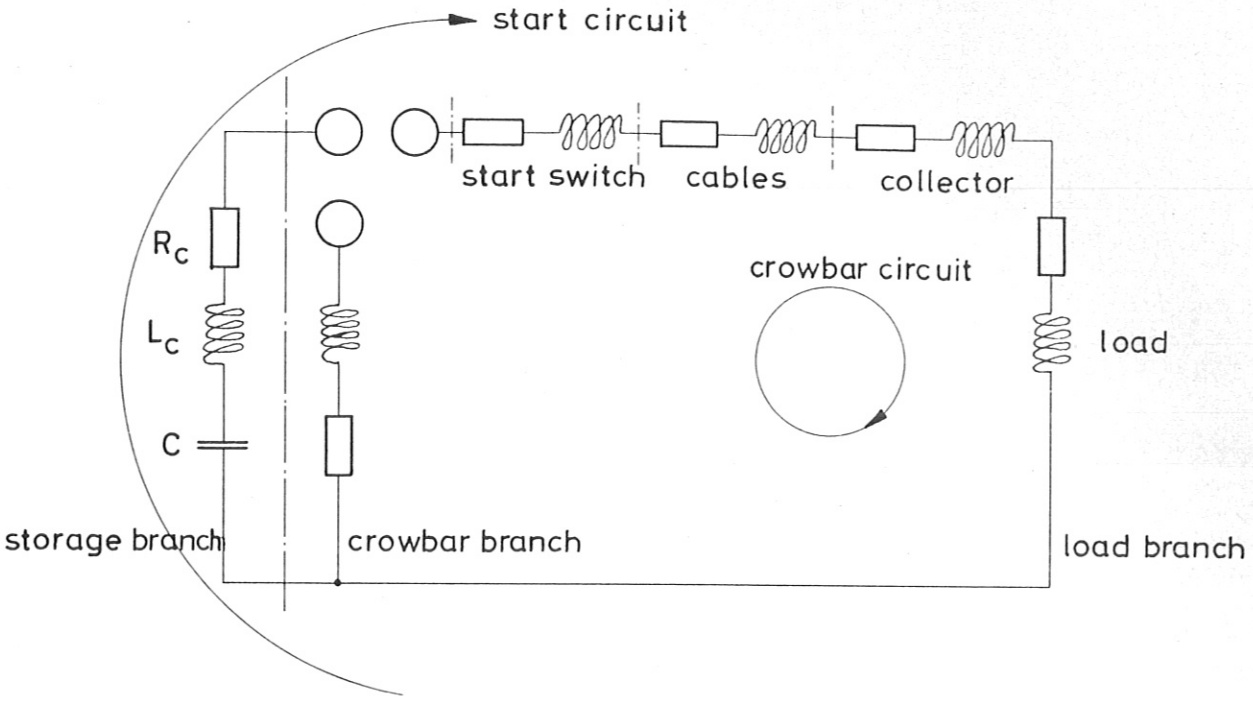

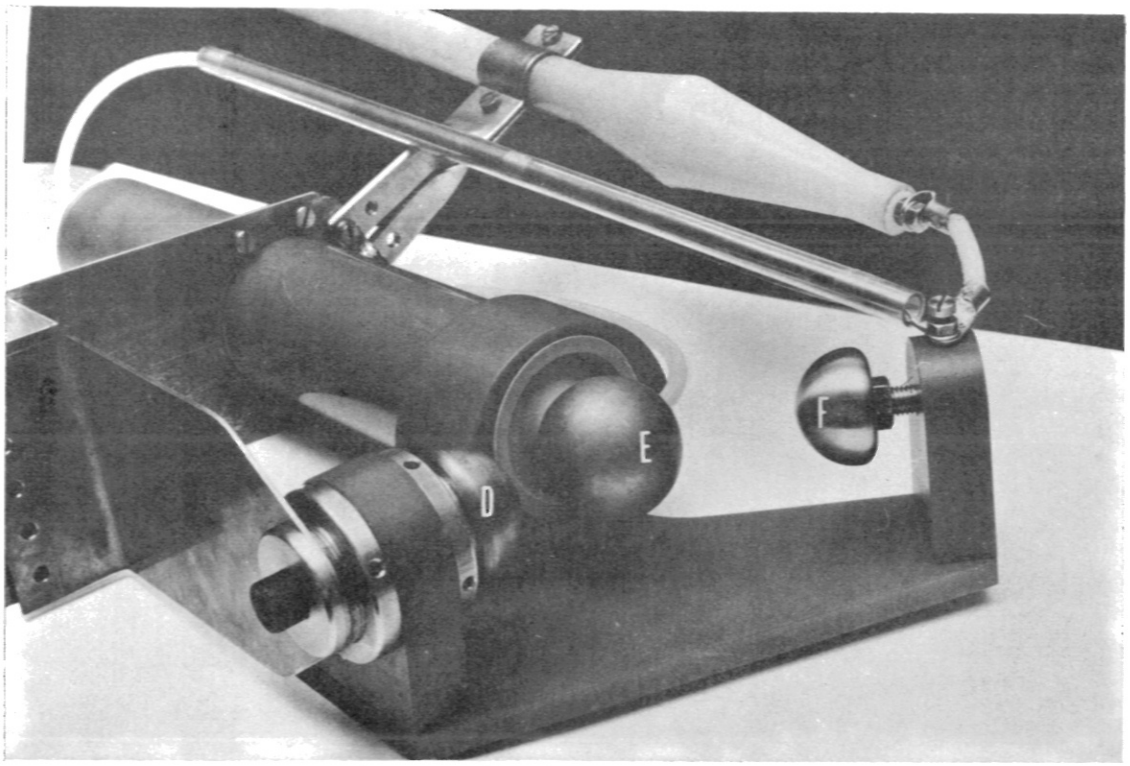

a) Principle Data of a High Current Capacitor Bank
b) Crowbar Spark Gap I

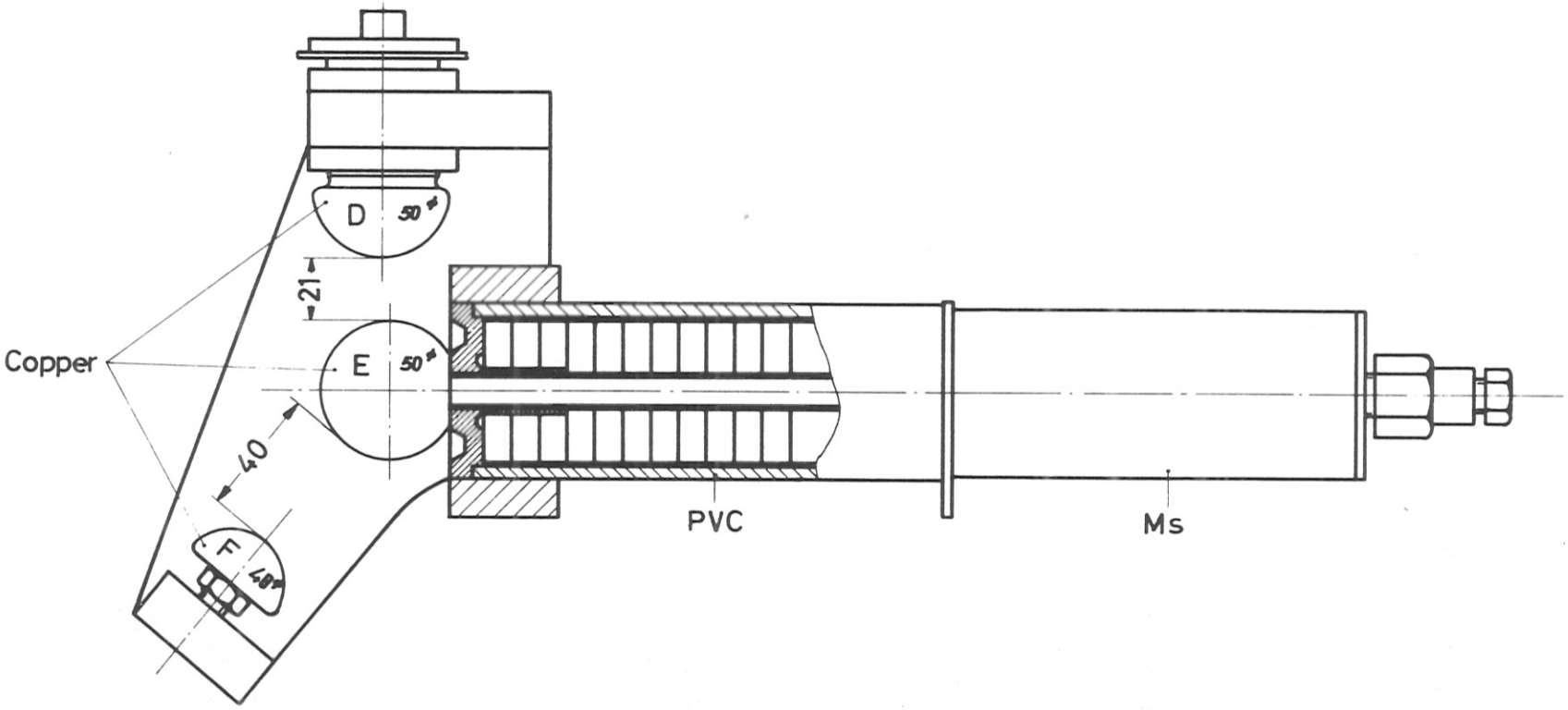

Section Drawing Spark Gap I

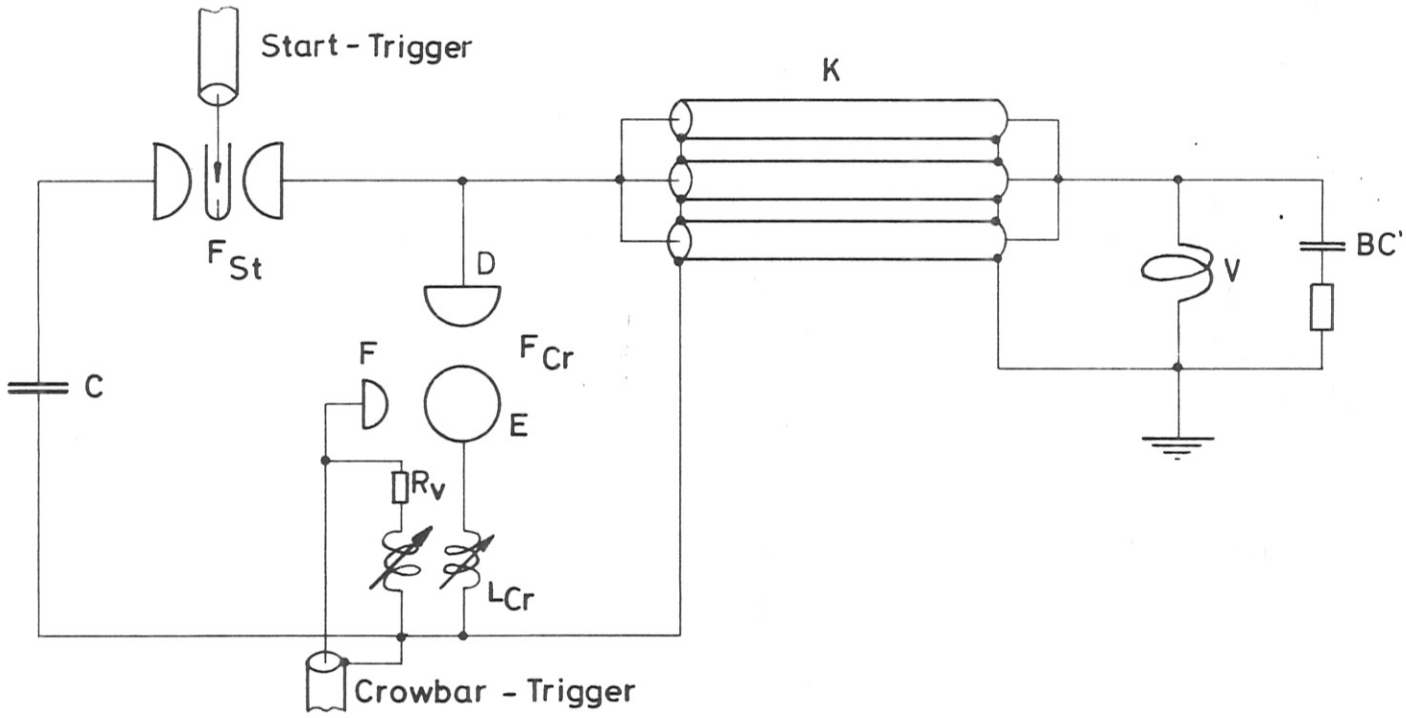

C	Capacitor 10,6 kJ ; 13,3 µF ; 40 kV	L_C	= 0,022 µH	R_C	= 10 mΩ
F_{St}	Start Spark Gap	L_{FSt}	= 0,20 µH	R_{FSt}	= 1,3 mΩ
K	Cable	L_K	= 0,25 µH	R_K	= 10,6 mΩ
V	Load	L_V	= 2,6 µH	R_V	= 1 mΩ
BC	R-C-Transient-Unit	L_{BC}	= 0,02 µH	R_{BC}	= 1,09 Ω
F_{Cr}	Crowbar Spark Gap	L_{FCr}	= 0,19 µH	R_{FCr}	= 9 mΩ
	Connections	L_A	= 0,14 µH	R_A	= 2 mΩ
	Crowbar Branch	$L_{FCr} + L_A$	= 0,33 µH	$R_{FCr} + R_A$	= 11 mΩ

Principle Data of Crowbar Spark Gap I

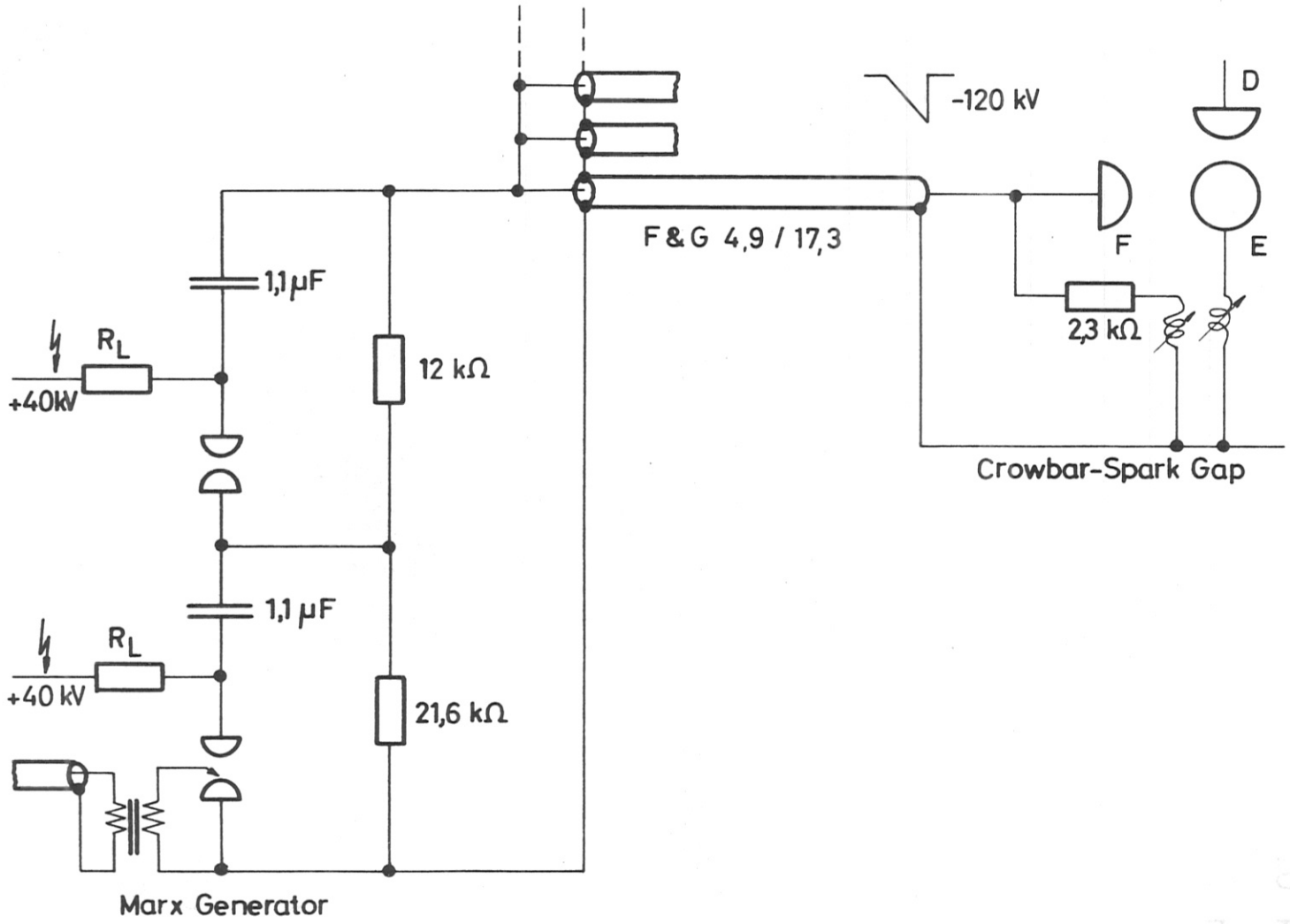

Triggercircuit of Crowbar Spark-Gap I

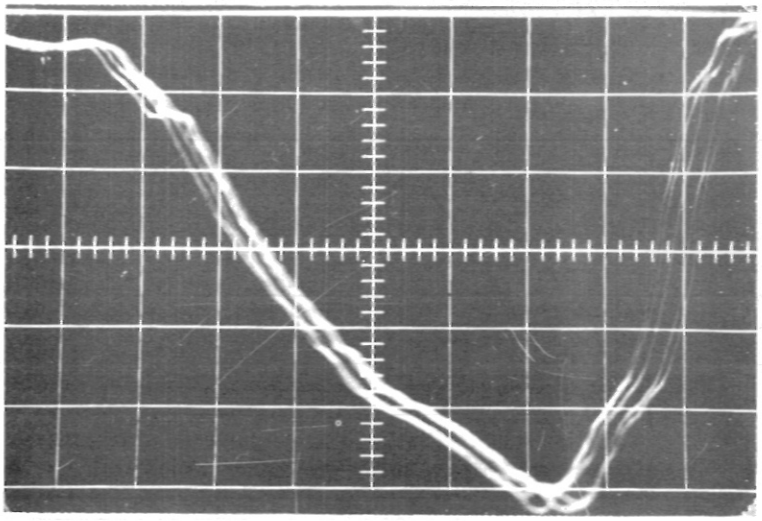

Voltage at electrode F

20 kV/cm

50 ns/cm

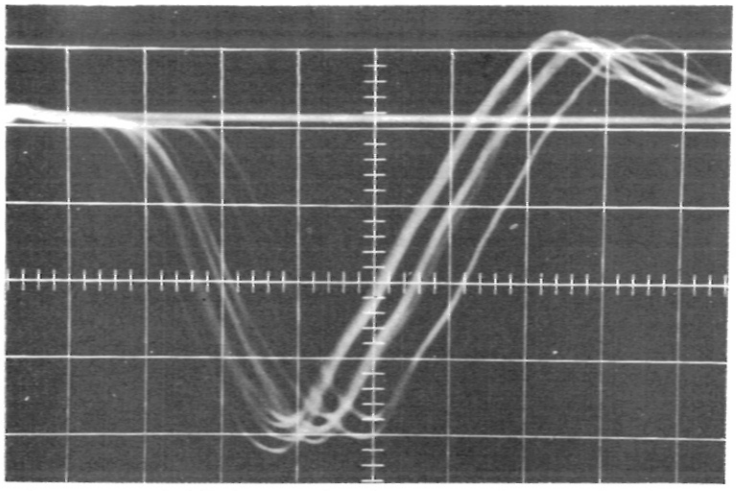

Voltage at electrode E
without premagnetisation

16,5 kV/cm

20 ns/cm

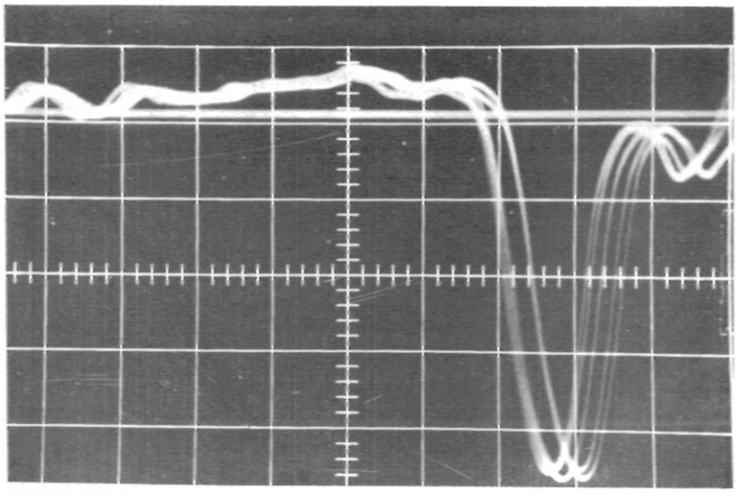

Voltage at electrode E
with premagnetisation

16,5 kV/cm

50 ns/cm

Voltage at the Electrodes
F, E

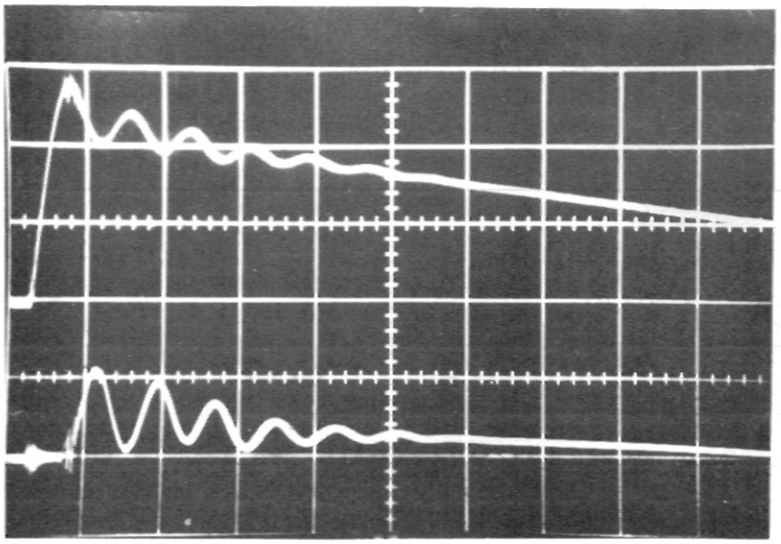

current in the load

20 µs/cm

current in crowbar circuit

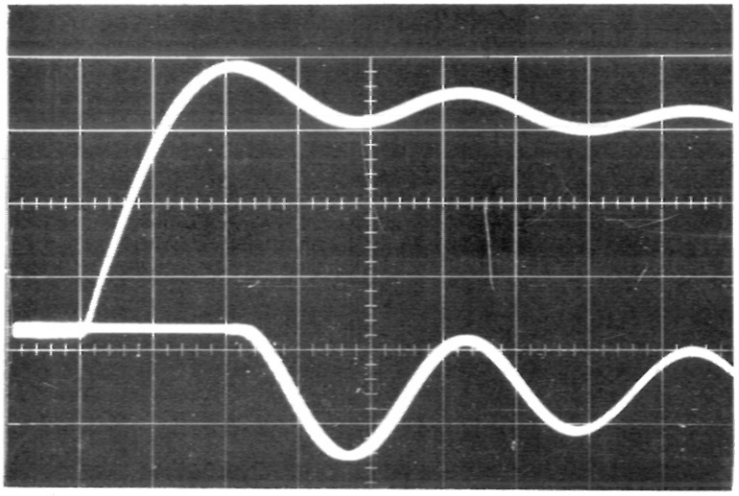

current in the load

5 µs/cm

current in crowbar circuit

shot no. 10....30

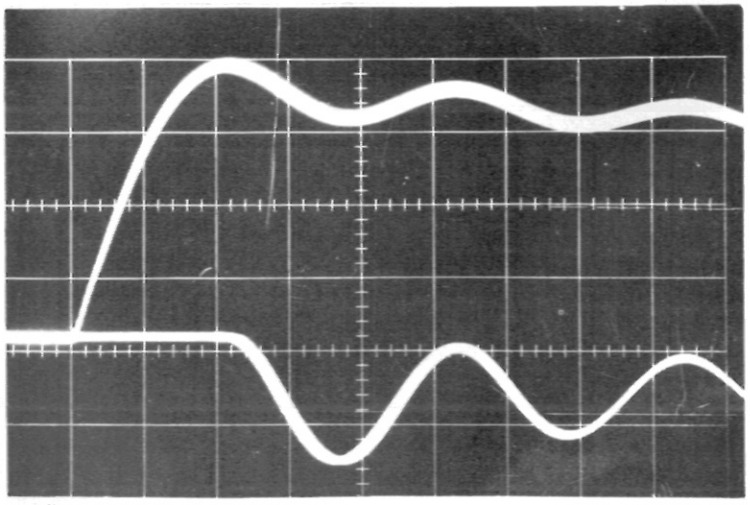

current in the load

5 µs/cm

current in crowbar circuit

shot no. 7980....8000

Current in the Load

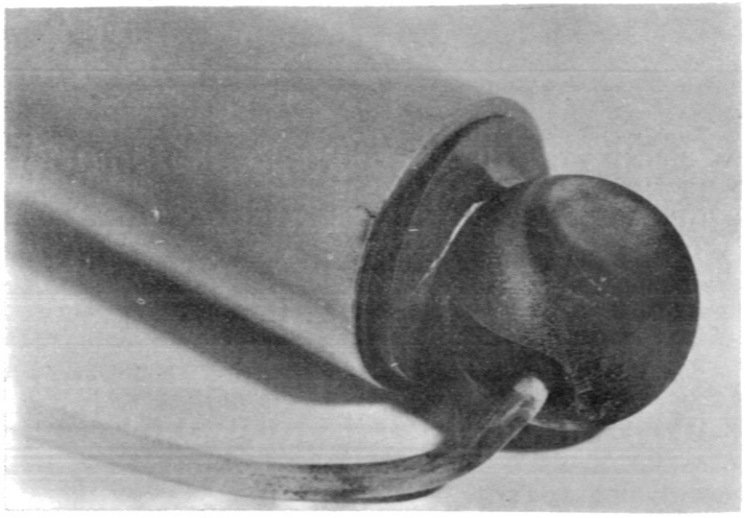

Crowbar cathode
after 8000 shots

Material copper, i_{max} : 80 k amps
W : 10,6 kJ
Q : 12 C

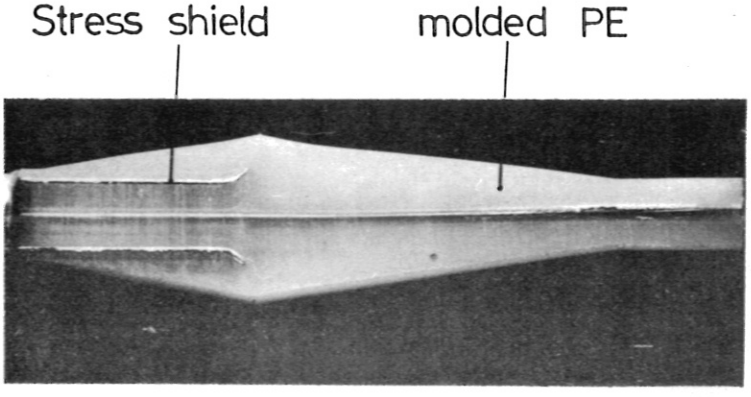

Termination of molded PE for 150 kV

Crowbar Electrodes after 8000 Shots

Trigger Cable Termination

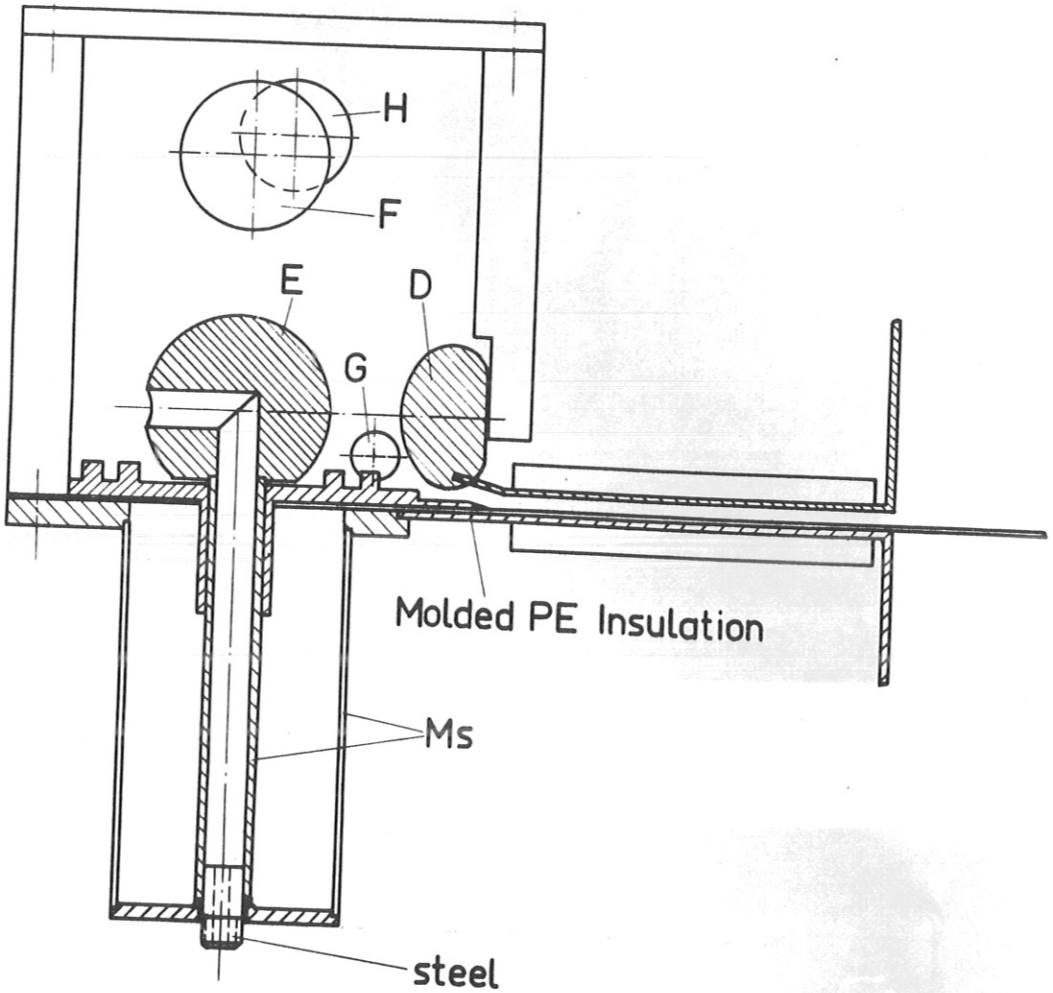

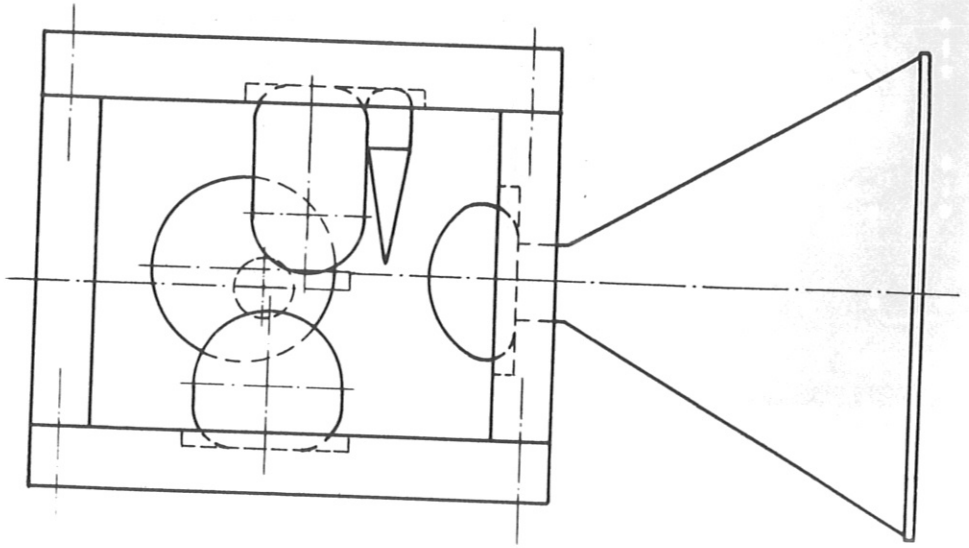

Section Drawing Crowbar Spark Gap
II

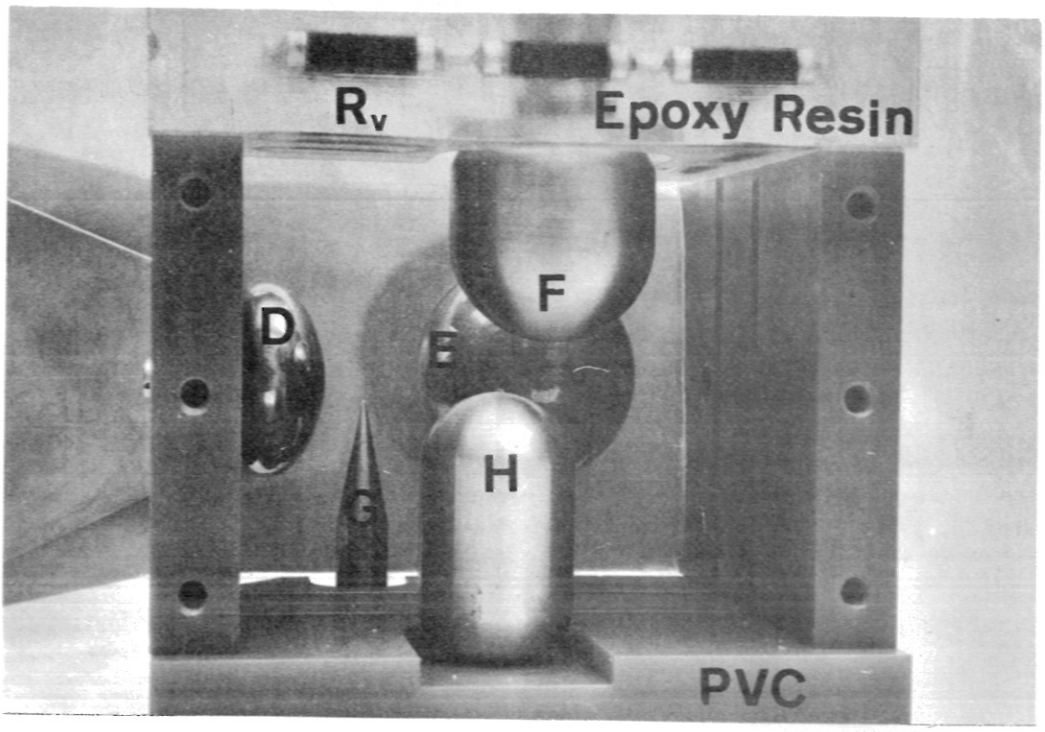

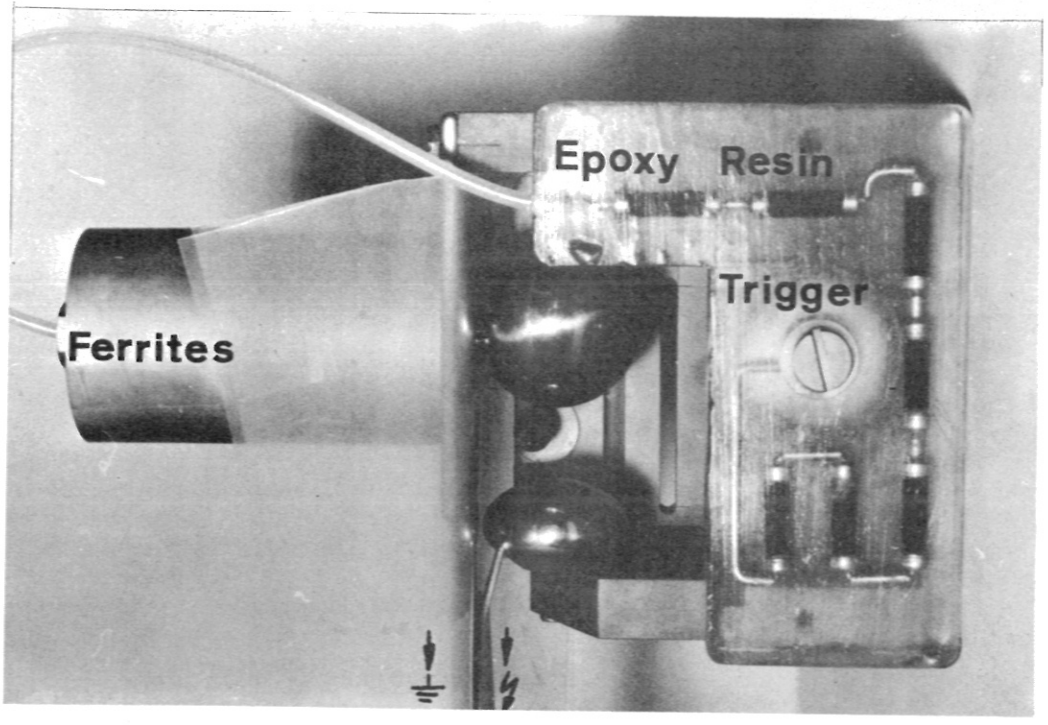

Fotos of Crowbar Spark Gap II

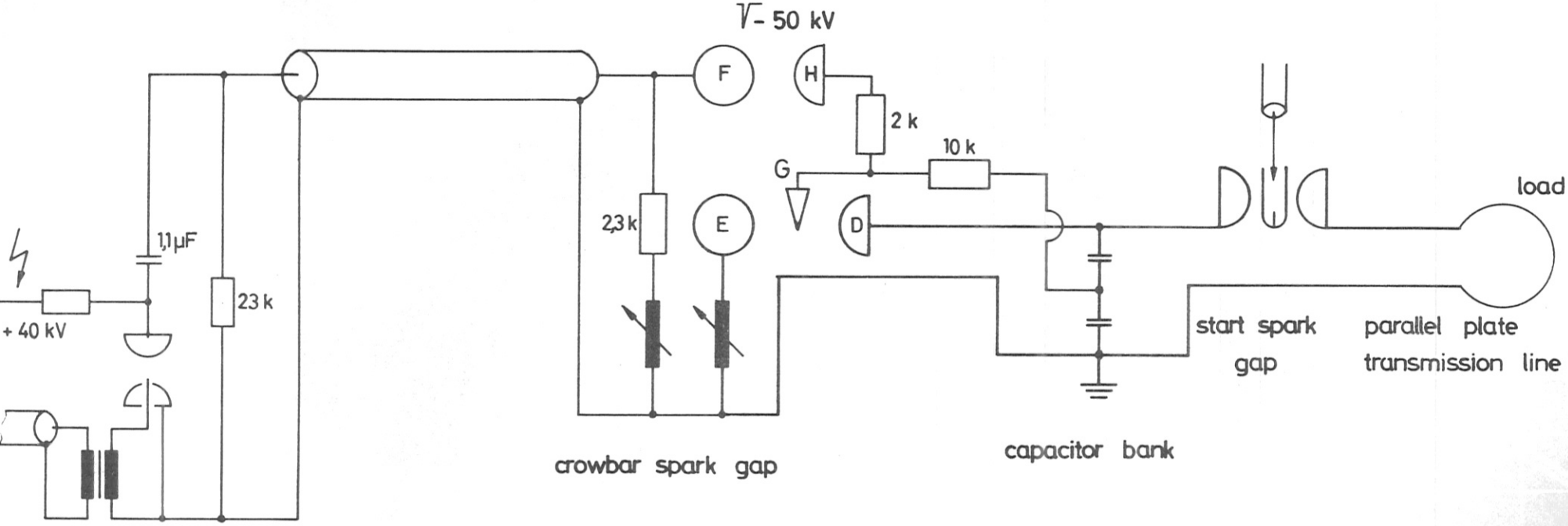

capacitor bank 5,4 kJ; 6,68 µF; 40 kV L_c = 0,044 µH; R_c = 20 mΩ

start spark gap L_{FSt} = 0,019 µH; R_{FSt} = 5 mΩ

parallel plate transmission line + load L = 0,377 µH; R = 8 mΩ

crowbar spark gap L_{Cr} = 0,065 µH; R = 5 mΩ

Principle Data of Crowbar Spark Gap II

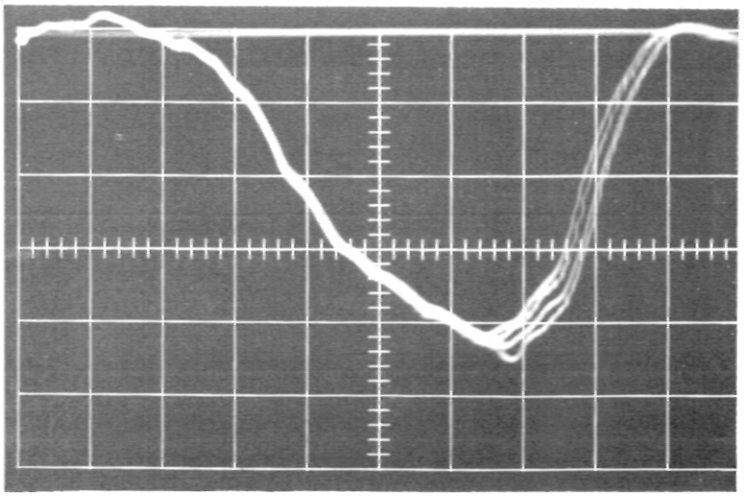

Voltage at electrode F

50 ns/cm

11,9 kV/cm

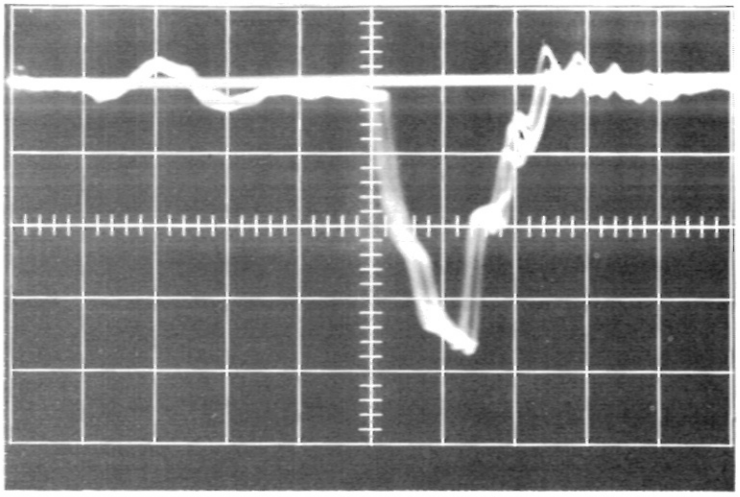

Voltage at electrode G

50 ns/cm

8,9 kV/cm

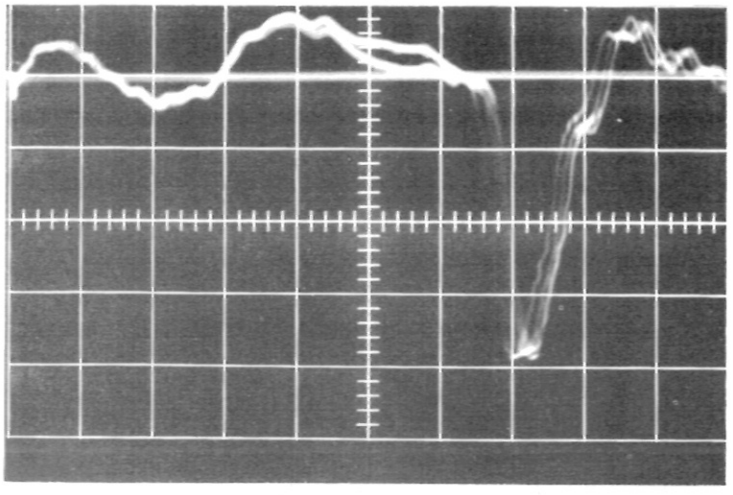

Voltage at electrode E

50 ns/cm

8,9 kV/cm

Crowbar Spark Gap II
Voltage at the Electrodes F, G and E

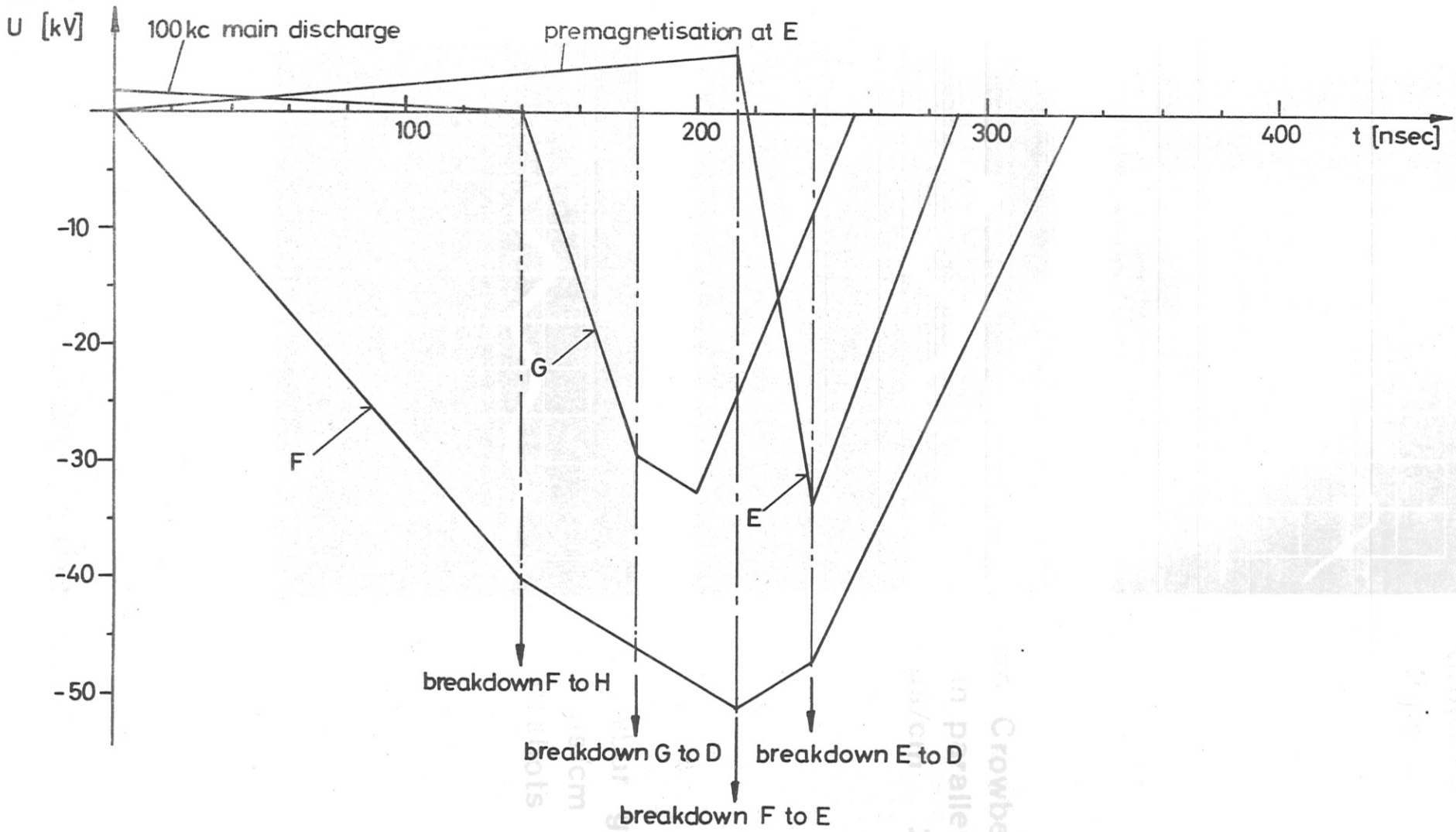

Idealised Voltage Waveform at the Electrodes E, F and G

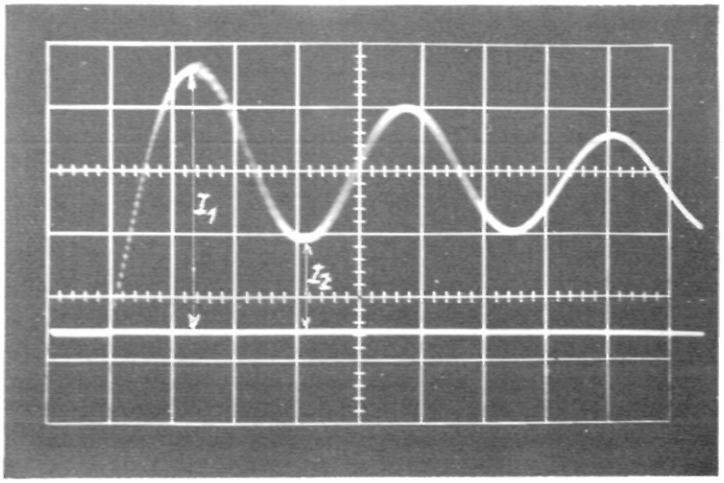

Crowbar gap I
2 μs/cm

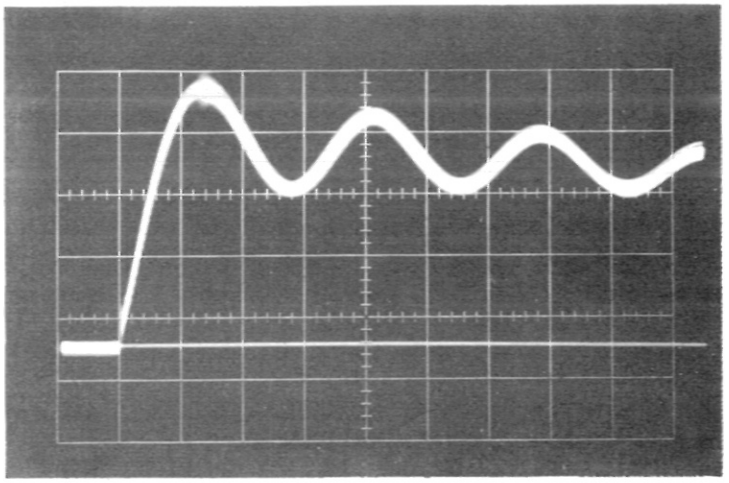

Two Crowber gaps I
in parallel
2 μs/cm 20 shots

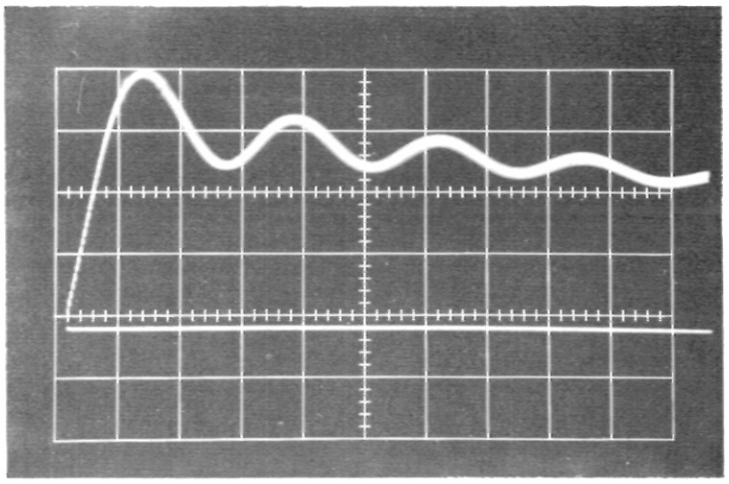

Crowbar gap II
2 μs/cm
20 shots

Current in the Load

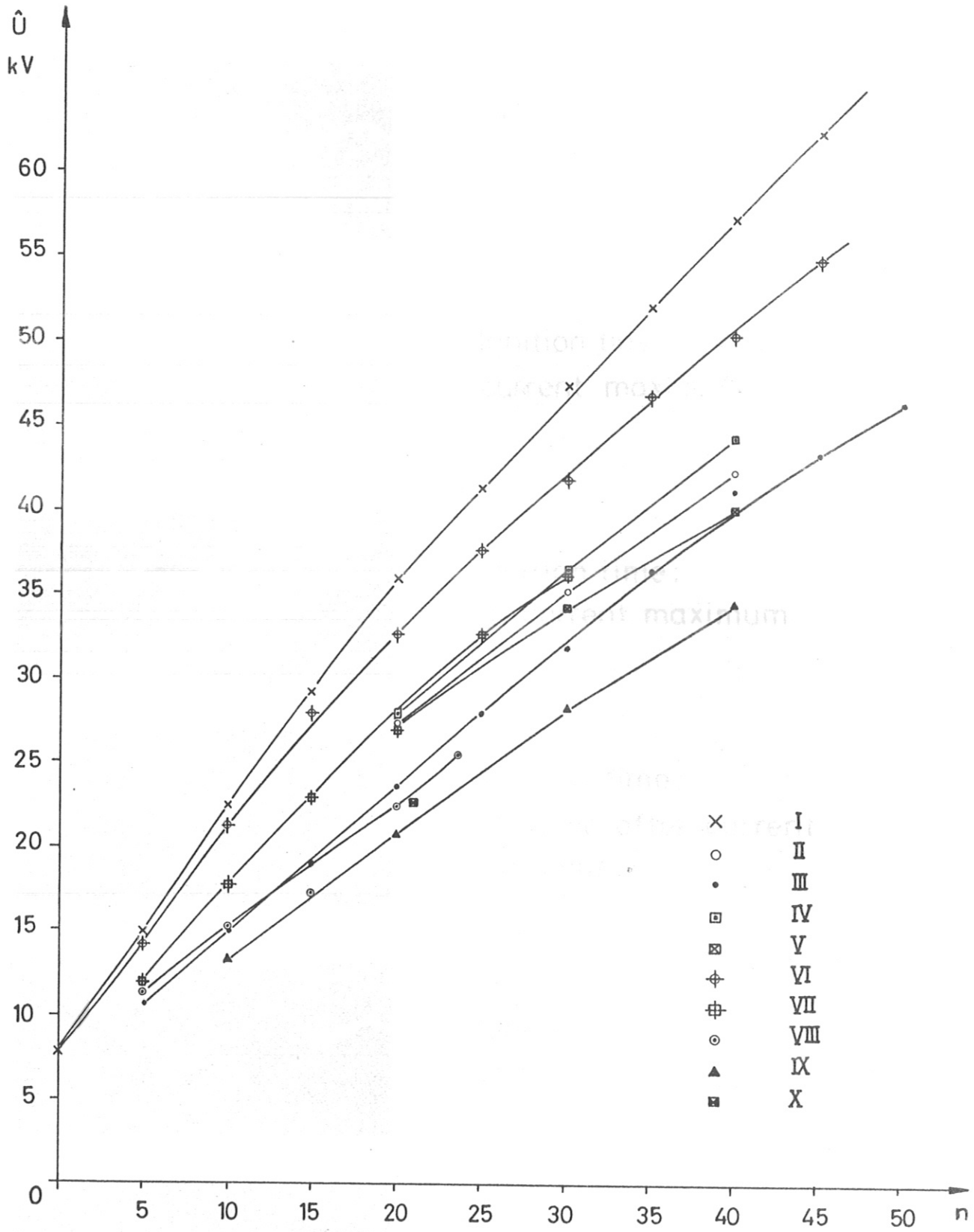

Measurements on Ferrite-Cores

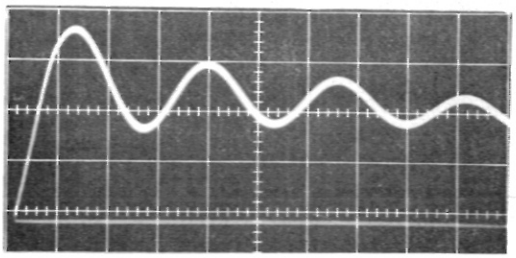

Ignition time: 200 n sec befor current maximum.

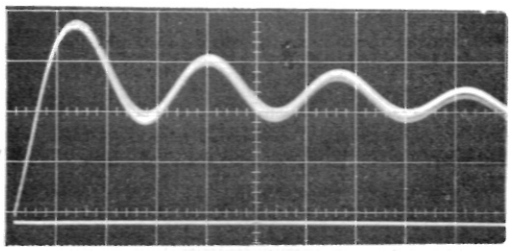

Ignition time: 100 n sec before current maximum.

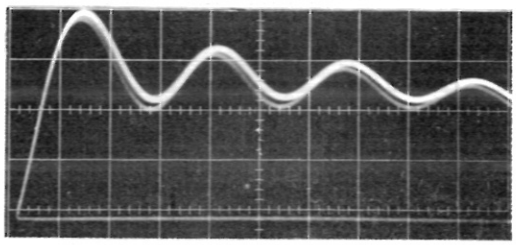

Ignition time:
at current maximum

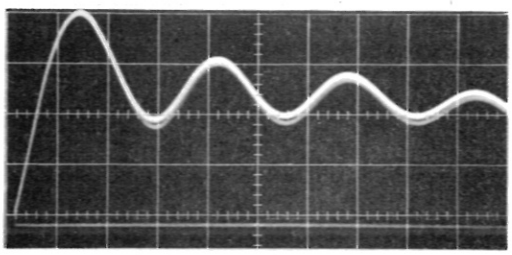

Ignition time:
100 n sec after current maximum

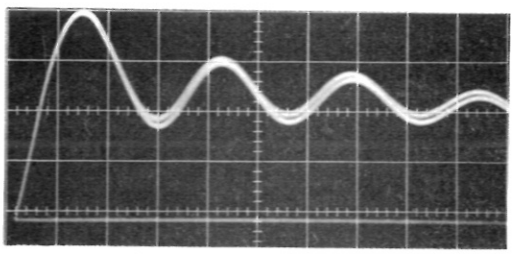

Ignition time :
200 n sec after current max.

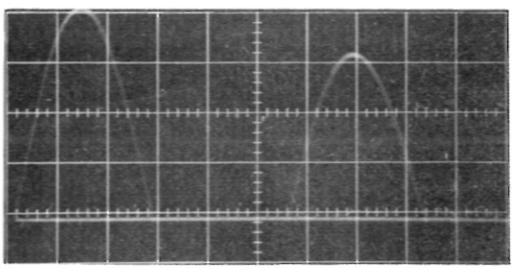

Oscillating

Spark gap III : Used for crowbar switching. Current in the load.
Time base 2 μ sec/div. 5 shots.